Apparent lack of physical or functional interaction between $Ca_V1.1$ and its distal C terminus

Joshua D. Ohrtman,[1] Christin F. Romberg,[2] Ong Moua,[1] Roger A. Bannister,[2] S. Rock Levinson,[1] and Kurt G. Beam[1]

[1]Department of Physiology and Biophysics and [2]Department of Medicine-Cardiology Division, University of Colorado, Denver, Aurora, CO 80045

$Ca_V1.1$ acts as both the voltage sensor that triggers excitation–contraction coupling in skeletal muscle and as an L-type Ca^{2+} channel. It has been proposed that, after its posttranslational cleavage, the distal C terminus of $Ca_V1.1$ remains noncovalently associated with proximal $Ca_V1.1$, and that tethering of protein kinase A to the distal C terminus is required for depolarization-induced potentiation of L-type Ca^{2+} current in skeletal muscle. Here, we report that association of the distal C terminus with proximal $Ca_V1.1$ cannot be detected by either immunoprecipitation of mouse skeletal muscle or by colocalized fluorescence after expression in adult skeletal muscle fibers of a $Ca_V1.1$ construct labeled with yellow fluorescent protein (YFP) and cyan fluorescent protein on the N and C termini, respectively. We found that L-type Ca^{2+} channel activity was similar after expression of constructs that either did (YFP-$Ca_V1.1_{1860}$) or did not (YFP-$Ca_V1.1_{1666}$) contain coding sequence for the distal C-terminal domain in dysgenic myotubes null for endogenous $Ca_V1.1$. Furthermore, in response to strong (up to 90 mV) or long-lasting prepulses (up to 200 ms), tail current amplitudes and decay times were equally increased in dysgenic myotubes expressing either YFP-$Ca_V1.1_{1860}$ or YFP-$Ca_V1.1_{1666}$, suggesting that the distal C-terminal domain was not required for depolarization-induced potentiation. Thus, our experiments do not support the existence of either biochemical or functional interactions between proximal $Ca_V1.1$ and the distal C terminus.

The Journal of General Physiology

INTRODUCTION

In response to action potential–induced depolarization, $Ca_V1.1$ serves in skeletal muscle as the voltage-sensing apparatus that initiates excitation–contraction coupling and additionally produces L-type Ca^{2+} current (Tanabe et al., 1988). Two distinct sizes of $Ca_V1.1$ polypeptide have been identified in adult rabbit skeletal muscle (De Jongh et al., 1991). The first, an ∼212-kD full-length translation product, is less abundant than the ∼175-kD form that is produced posttranslationally from the full-length protein by cleavage of the C terminus. Via mass spectrometry, the site of cleavage has been found to occur between alanine1664 and asparagine1665 (Hulme et al., 2005). Additionally, analysis of $Ca_V1.1$ fragments expressed in tsA-201 and yeast cells led to the hypothesis that the cleaved distal C terminus remains noncovalently associated with the rest of the channel (Hulme et al., 2005), and that the binding of an A kinase–anchoring protein (AKAP)15 to a modified leucine zipper within the distal C terminus recruits PKA to the $Ca_V1.1$-containing channel complex (Hulme et al., 2002). Comparable experiments suggested that a similar arrangement might occur in cardiac muscle between $Ca_V1.2$ and its distal C terminus (De Jongh et al., 1996; Hulme et al., 2006), and between its distal C terminus, AKAP15, and PKA (Hulme et al., 2003).

The functional consequences of C-terminal truncation have been examined by heterologous expression of full-length and truncated $Ca_V1.1$ and $Ca_V1.2$ constructs. In *Xenopus laevis* oocytes, where the posttranslational proteolytic cleavage of the full-length proteins presumably does not occur, constructs encoding full-length $Ca_V1.1$ (Morrill and Cannon, 2000) and $Ca_V1.2$ (Wei et al., 1994) have lower estimated open probability (P_o) than those encoding the truncated proteins. In tsA-201 cells, for which it has been directly demonstrated that full-length $Ca_V1.2$ is not proteolytically cleaved (Hulme et al., 2006), full-length $Ca_V1.2$ likewise has lower P_o than truncated constructs (Gao et al., 2001; Hulme et al., 2006). Based on these and other results, it has been proposed that the distal C terminus functions as an autoinhibitory subunit of both $Ca_V1.1$ (Hulme et al., 2005) and $Ca_V1.2$ (Hulme et al., 2006). Furthermore, it has been proposed that this autoinhibition is relieved for $Ca_V1.2$ in cardiomyocytes by activation of the β-adrenergic pathway (Fuller et al., 2010), and for $Ca_V1.1$ in skeletal muscle cells in response to strong depolarization.

Correspondence to Kurt G. Beam: kurt.beam@ucdenver.edu

Abbreviations used in this paper: AKAP, A kinase–anchoring protein; FDB, flexor digitorum brevis; P_o, open probability.

The Rockefeller University Press $30.00
J. Gen. Physiol. Vol. 145 No. 4 303–314
www.jgp.org/cgi/doi/10.1085/jgp.201411292

Depolarization-induced potentiation is displayed by L-type Ca^{2+} currents produced both by $Ca_V1.1$ (Sculptoreanu et al., 1993b; Johnson et al., 1994, 1997) and $Ca_V1.2$ (Pietrobon and Hess, 1990; Sculptoreanu et al., 1993a). Moreover, it has been suggested that this potentiation contributes to increased entry of Ca^{2+} per action potential in response to increased firing rate in both skeletal (Sculptoreanu et al., 1993b) and cardiac (Sculptoreanu et al., 1993a) muscle. Analysis of single-channel currents for $Ca_V1.2$ has shown that strong and/or prolonged depolarization causes the channel to enter a state with increased open dwell time, which has been termed "mode 2" gating (Pietrobon and Hess, 1990). At the macroscopic level, this entry into mode 2 gating has the consequence that increasing the amplitude or duration of a depolarizing pulse causes the tail currents that result from a subsequent repolarization both to be larger and to decay more slowly.

In contrast to the results obtained in nonmuscle cells, we earlier found (Beam et al., 1992) that P_o did not differ for full-length or truncated $Ca_V1.1$ constructs after expression in dysgenic myotubes (null for endogenous $Ca_V1.1$), which raises the possibility that the $Ca_V1.1$ distal C terminus might not function in an autoinhibitory manner within a native skeletal muscle environment. Thus, in the experiments described here, we have reexamined, in skeletal muscle cells, the posttranslational truncation of $Ca_V1.1$ and its functional consequences. The experiments made use of immunoprecipitation of native $Ca_V1.1$ in neonatal mouse muscle, imaging of fluorescently tagged $Ca_V1.1$ constructs expressed in adult mouse muscle in vivo, and functional analysis of full-length or truncated constructs after expression in dysgenic myotubes. The results do not support the idea that the distal C terminus is required for depolarization-induced potentiation or that it associates noncovalently with proximal $Ca_V1.1$.

MATERIALS AND METHODS

Myotube cultures, Western blotting, and immunoprecipitation

Normal and dysgenic myotubes were cultured as described previously (Tanabe et al., 1988; Beam and Franzini-Armstrong, 1997). For biochemical measurements, the dissociated myoblasts were plated at a density of 2×10^6 per 10–cm dish and for electrophysiology at a density of 10^5 within an ~1-cm circle scratched into the bottom of a 35-mm dish. To prepare myotube membranes, a 3× rinse of the 10-cm culture dishes with Ca^{2+}-Mg^{2+} free rodent Ringer's solution (mM: 155 NaCl, 5 KCl, and 10 HEPES, pH 7.4, with NaOH) was followed by the addition of 1 ml of 0.3% digitonin in detergent buffer (mM: 100 NaCl and 50 Tris-HCl, pH 7.4). The myotubes were scraped from the dish with a rubber policeman and then homogenized (see below).

Fore- and hind-limb muscle were dissected on ice from mice of varying ages, frozen on dry ice, stored at −80°C, and subsequently homogenized with an Ultra-Turrax (Janke and Kunkel) in an ice-cold buffer (mM: 20 $Na_4P_2O_7$, 20 NaH_2PO_4, 2.5 EGTA, and 300 sucrose) containing protease inhibitors (μg/ml: 10 aprotinin, 190 iodoacetamide, 50 N-α-tosyl-L-lysine chloromethyl ketone hydrochloride, 10 leupeptin, 40 phenylmethanesulfonyl-fluoride, 100 benzamidine, 14 pepstatin A, and 2 antipain). The homogenate was centrifuged at 1,500 *g* for 10 min at 4°C, and the supernatant was collected and pooled with the supernatant that resulted when the pellet was resuspended and subjected to the same centrifugation. Membranes in the pooled supernatants were pelleted by centrifugation at 100,000 *g* at 4°C for 60 min and resuspended in 1% digitonin in detergent buffer. Both the muscle membranes and the scraped myotubes (see above) were subjected to 15 passes with a type A pestle in a Dounce homogenizer (Bellco Glass), and then kept on ice for an additional 30 min, followed by centrifugation at 100,000 *g* at 4°C to pellet insoluble material. Aliquots for SDS PAGE were denatured in Laemmli sample buffer with 5% β-mercaptoethanol and placed in a boiling water bath for 30 s.

The IIF7 monoclonal antibody (Leung et al., 1987) was provided by K. Campbell (University of Iowa School of Medicine, Iowa City, IA). Aliquots of the lyophilized ascites were reconstituted to their original volume and stored at −20°C before use. To generate the distal antibody, a polypeptide corresponding to residues 1,819–1,834 of $Ca_V1.1$ (compare Fig. 1), with a cysteine added to the N terminus, was synthesized and purified by HPLC and, after conjugation to maleimide-activated keyhole limpet hemocyanin (Thermo Fisher Scientific), was used to immunize rabbits (procedures performed by the Macromolecular Resource Facility at Colorado State University). The antibody was purified by means of an affinity column containing agarose beads (Pierce SulfoLink; Thermo Fisher Scientific) to which the immunizing peptide had been conjugated by its N-terminal cysteine. The resulting antibody was ineffective for Western blotting but was effective for immunoprecipitation. For blocked antibody experiments, the distal antibody was incubated for 2 h at room temperature with 200 μg of the immunizing peptide to a final peptide/antibody molar ratio of 100:1.

For immunoprecipitation, the solubilized muscle and myotube membranes were diluted to reduce the concentration of digitonin to 0.1% in detergent buffer and mixed with the antibodies: 85 μg/ml of the distal antibody or 1:50 of IIF7 ascites (for IIF7, SDS was also present at a final concentration of 0.2%). After overnight incubation at 4°C with rotational mixing, protein G agarose, which had been equilibrated with the immunoprecipitation buffer, was added at 50 μl/ml, and rotational mixing continued for an additional 4–6 h. The beads were spun down at 1,500 *g* for 5 min. The pellet was then washed twice, resuspended in Laemmli sample buffer containing 5% β-mercaptoethanol, placed in a boiling water bath for 2 min, and cooled and centrifuged in an Eppendorf microfuge for 5 min at 10,000 rpm, and the supernatant was retained.

Electrophoresis was performed on a 5% gel, followed by wet transfer to a nitrocellulose membrane (50 V for 2 h). After a 2-h incubation in blocking buffer (5% wt/vol nonfat dry milk in Tris-buffered saline, pH 7.4, with 0.1% tween [TBS-T]), the membrane was incubated overnight in blocking buffer with 1:5,000 IIF7 ascites fluid, washed once for 15 min and four times for 5 min in TBS-T, incubated in 1:5,000 horseradish peroxidase–conjugated goat anti–mouse IgG for 90 min, and visualized by means of enhanced chemiluminescence.

cDNA constructs

The construction of the plasmids YFP-$Ca_V1.1_{1860}$ (YFP, 15-residue linker, rabbit $Ca_V1.1$ residues 1–1,860, 14 nonnative residues, and a stop), YFP-$Ca_V1.1_{1666}$ (YFP, 15-residue linker, $Ca_V1.1$ residues 1–1,666, 13 nonnative residues, and a stop), CFP-YFP-$Ca_V1.1$ (CFP, 23-residue linker, YFP, 15-residue linker, $Ca_V1.1$ residues 1–1,860, 14 nonnative residues, and a stop), and YFP-$Ca_V1.1$-CFP (YFP, 15-residue linker, $Ca_V1.1$ residues 1–1,860, 13 nonnative residues, and CFP) was essentially as described previously (Lorenzon

et al., 2004; Papadopoulos et al., 2004). Full-length rabbit $Ca_V1.1$ has 1,873 residues (SwissProt accession no. P07293; Tanabe et al., 1987).

In vivo electroporation, dissociation, and imaging of flexor digitorum brevis (FDB) fibers

cDNA plasmids were delivered to FDB fibers of anesthetized 3-mo-old male C57BL/6J mice (The Jackson Laboratory) via an in vivo electroporation protocol similar to that originally described by DiFranco et al. (2007). In brief, the FDB muscle was injected via a 30-gauge needle with 10 µl of 2 mg/ml hyaluronidase solution and 1 h later with 20 µl cDNA (3–5 µg/µl). 5 min later, cDNAs were electroporated into the muscle with 20 100-V, 20-ms pulses delivered at 1 Hz via two gold-plated acupuncture needles (TCG20 × 25; Lhasa OMS) placed subcutaneously near the proximal and distal tendons (~10 mm apart). Transfected and nontransfected FDB muscles were dissected in cold rodent Ringer's solution (mM: 146 NaCl, 5 KCl, 2 $CaCl_2$, 1 $MgCl_2$, and 10 HEPES, pH 7.4 with NaOH). Muscles were then digested in 2% collagenase (Roche) in minimum essential medium (Gibco) with 10% fetal bovine serum (Hyclone) with agitation at 37°C for ~60 min. Immediately after digestion, the collagenase solution was replaced with minimum essential medium without collagenase, and the muscles were triturated gently with a series of fire-polished glass pipettes of descending bore. Dissociated FDB fibers were allowed to settle onto laminin-coated 35-mm culture dishes with glass coverslip bottoms (MatTek) for 1–4 h at 37°C, 5% CO_2.

The dissociated transfected fibers were imaged in rodent Ringer's solution with either an LSM510 or LSM710 confocal microscope (Carl Zeiss). For CFP, excitation was either 458 nm (LSM510) or 440 nm (LSM710), and emission was either 465–495 nm (LSM510) or 455–495 nm (LSM710). For YFP, excitation was 514 nm, and emission was either 530 nm long-pass (LSM510) or 520–580 nm (LSM710). For quantitative comparison of fluorescence emission intensities between cells, the photomultiplier gains were kept identical, although it was usually necessary to vary the laser excitation intensities to obtain good images. Control experiments demonstrated that the ratio of (fluorescence intensity)/(laser intensity) was constant as long as there was no saturation of the A/D converter. Thus, before comparison, fluorescence intensities were scaled offline to account for differences in laser excitation.

Electrophysiological analysis of endogenous $Ca_V1.1$ in normal muscle cells, and YFP-$Ca_V1.1_{1860}$ and YFP-$Ca_V1.1_{1666}$ in dysgenic myotubes

Dysgenic myotubes, which lack endogenous $Ca_V1.1$ (Knudson et al., 1989), were microinjected (Beam and Franzini-Armstrong, 1997) in single nuclei with 200 ng/µl cDNA for YFP-$Ca_V1.1_{1860}$ or YFP-$Ca_V1.1_{1666}$. Expressing cells were positively identified 48 h after injection by yellow fluorescence.

Macroscopic currents were obtained using the whole-cell patch-clamp technique (Hamill et al., 1981). Patch pipettes, which were constructed using borosilicate glass and filled with an "internal solution" (mM: 140 CsAsp, 5 $MgCl_2$, 10 Cs_2EGTA, and 10 HEPES, pH 7.4 with CsOH), had resistances of 1.7–2.2 MΩ for myotubes and <1 MΩ for dissociated FDB fibers. Although the internal solution lacked ATP, myotubes subjected to whole-cell patch clamping with this solution retain the ability for upwards of 30 min to release Ca^{2+} from the sarcoplasmic reticulum and to resequester it (Bannister et al., 2008), which implies the continuing presence of sufficient myoplasmic ATP to support robust activity of the sarcoplasmic reticulum Ca^{2+} pump. The external solution contained (mM): 10 $CaCl_2$, 145 tetraethylammonium-Cl, 0.003 tetrodotoxin, and 10 HEPES, pH 7.4 with tetraethylammonium-OH.

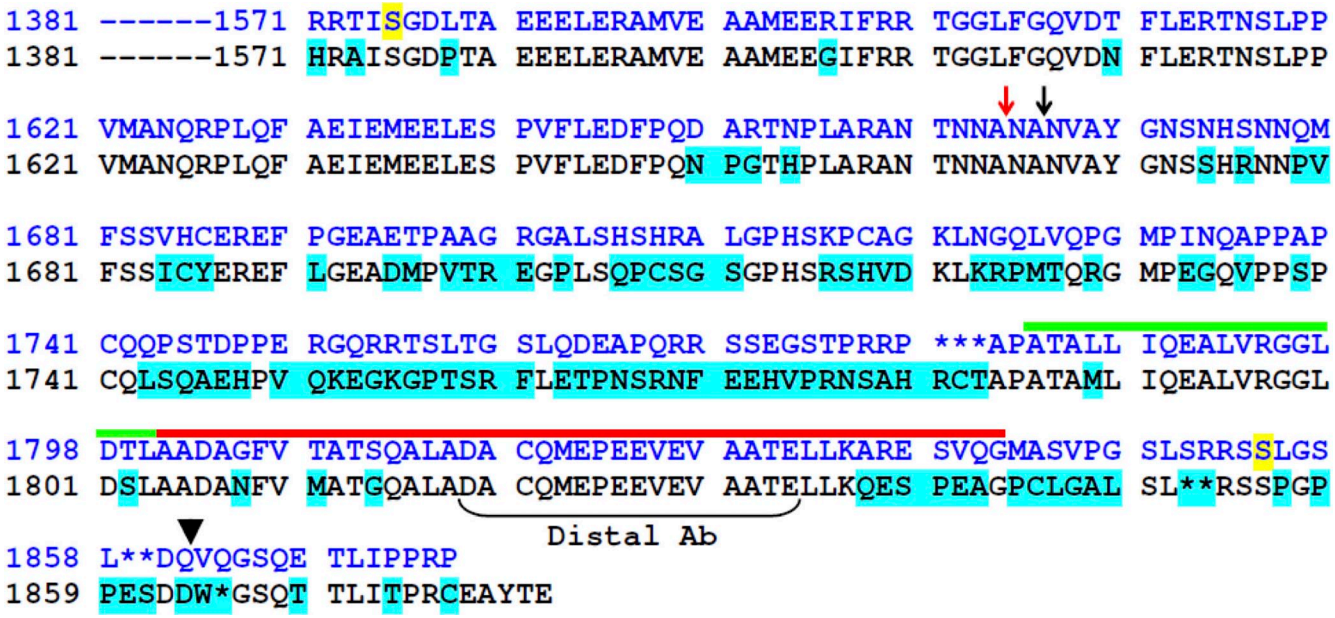

Figure 1. Alignment of C termini of $Ca_V1.1$ from rabbit (SwissProt accession no. P07293.1; blue font) and mouse (SwissProt accession no. Q02789), with introduced gaps indicated by asterisks. Residues 1,381–1,570 are identical for the two sequences. Residues of the mouse sequence that differ from those of rabbit are indicated by cyan highlighting. The sites of posttranslational truncation of rabbit $Ca_V1.1$ (Hulme et al., 2005) and the termination of rabbit sequence for our construct YFP-$Ca_V1.1_{1666}$ are indicated by red and black arrows, respectively. The black arrowhead indicates the final native residue of the constructs YFP-$Ca_V1.1_{1860}$ and YFP-$Ca_V1.1$-CFP, and the bracket indicates the peptide sequence used to generate the "Distal" antibody. The domains of the rabbit distal C terminus proposed to bind AKAP (Hulme et al., 2002, 2005) and to mediate binding to proximal $Ca_V1.1$ (distal C terminus interaction domain; Hulme et al., 2005) are indicated by green and red lines, respectively. Residues of rabbit $Ca_V1.1$ shown to be phosphorylated by PKA in vivo (Rotman et al., 1992; Emrick et al., 2010) are highlighted in yellow.

In myotubes, test currents were obtained by stepping from the holding potential (−80 mV) to −30 mV for 1 s (to inactivate endogenous T-type Ca^{2+} current) to −50 mV for 25 ms, and then to more positive test potentials; currents in FDB fibers were elicited by stepping directly from the holding potential to the test potential. Test currents were corrected for linear components of leak and capacitive current by digitally scaling and subtracting the average of eight control currents each elicited by a 20-mV hyperpolarization from the holding potential. The current evoked by a 20-mV hyperpolarizing step was also used to calculate linear cell capacitance. Calcium currents were sampled either at 1 kHz or, for tail currents, at 10 kHz, filtered at 0.5 and 5 kHz, respectively. Currents as a function of test potential were fitted according to:

$$I(V) = G_{max} * (V - V_{rev}) \Big/ \left\{1 + exp\left[-(V - V_{1/2}) / k\right]\right\}, \qquad (1)$$

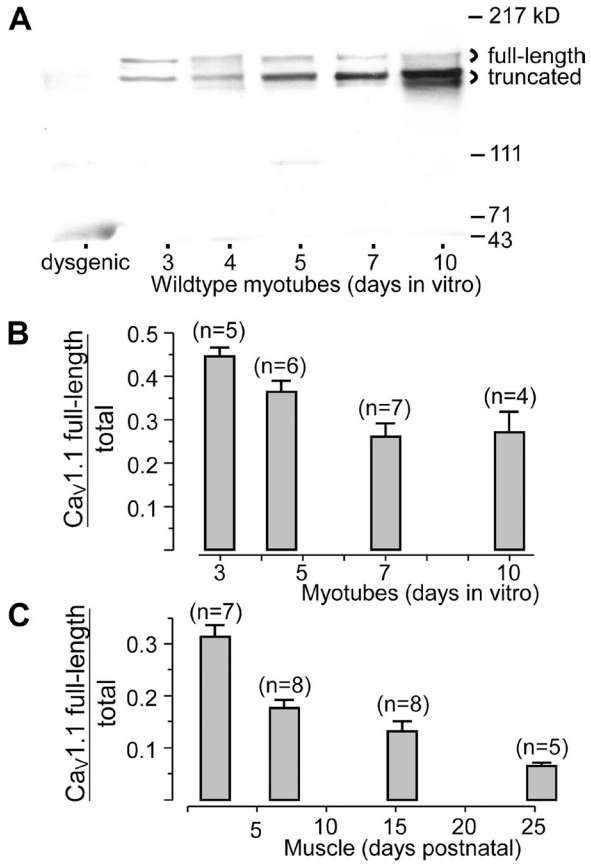

Figure 2. Developmental changes in expression of full-length and truncated $Ca_V1.1$. (A) Western blots of membranes isolated from wild-type myotubes grown in culture for the indicated number of days (denoting plating as "Day 1") and probed with the IIF7 monoclonal antibody, which recognizes both the full-length and truncated species. The leftmost lane illustrates membranes from dysgenic ($Ca_V1.1$-null) myotubes. Based on scanning densitometry, full-length $Ca_V1.1$ as a fraction of total (full-length plus truncated) is plotted as a function of developmental age in vitro (B) and in vivo (C). Error bars indicate SEM, and numbers of cultures or mice are indicated in parentheses. In B, myotubes from 4–5 d were grouped and plotted at day 4.5. In C, mice of 1–3, 5–9, 13–18, and 21–30 d, respectively, were grouped and plotted at time points corresponding to the average age of each group.

where $I(V)$ is the peak inward Ca^{2+} current measured at test potential V, G_{max} is the maximal Ca^{2+} conductance, V_{rev} is the reversal potential, $V_{1/2}$ is the potential for half-activation, and k is a slope factor.

Potentiation was assessed by measuring the peak amplitude (I) and half-decay time (T) of tail currents produced by repolarization after 200-ms test pulses ranging from 40 to 90 mV in 10-mV increments, or after a 90-mV depolarization ranging in duration from 50 to 200 ms in 50-ms increments. To ensure both that the tail current decay was complete within 20 ms, and that it was not so rapid that the tail currents could not be well resolved, the repolarization potential varied between cells (−20 mV for $Ca_V1.1_{1860}$, from −20 to −40 mV for $Ca_V1.1_{1666}$, and −30 mV for native $Ca_V1.1$). In individual cells, however, the relative changes in tail current amplitude and decay were always calculated as ratios for a single repolarization potential (e.g., the amplitude of the tail current after the 90-mV prepulse divided by the amplitude of the tail current after the 40-mV prepulse, both measured at the same repolarization potential). One would not expect these ratios to depend on the repolarization potential, but we directly verified this in control experiments on several cells. Cells were allowed to recover for ~2 s at −80 mV between each depolarization–repolarization combination.

Analysis

Figures were made using the software program SigmaPlot (version 11.0; SSPS Inc.). All data are presented as mean ± SEM. Statistical comparisons were made by unpaired, two-tailed t test or ANOVA (as appropriate), with $P < 0.05$ considered significant.

RESULTS

Developmental regulation of $Ca_V1.1$ C-terminal truncation

Fig. 1 illustrates an alignment of the $Ca_V1.1$ C terminus from rabbit and mouse skeletal muscle, together with an indication of regions that have been reported to be important for its posttranslational processing in rabbit. As an initial approach for investigating the posttranslational processing of $Ca_V1.1$ in mouse, we used the monoclonal antibody IIF7, which has an epitope mapped to residues 956–1,005 (Campbell, K.P., personal communication). Because this region differs between mouse and rat by only two residues and is upstream of the C-terminal truncation site (Fig. 1, red arrow), IIF7 would be predicted to detect $Ca_V1.1$ in mouse independent of any posttranslational processing of the C terminus. Consistent with this prediction, Western blots with IIF7 revealed that wild-type myotubes contain two sizes of $Ca_V1.1$ (Fig. 2 A), which differed in mass by about the amount expected (~20 kD) if C-terminal truncation in mouse occurred at the same site as in rabbit. Note that each of the two sized forms appeared to a variable extent as doublets, which we found to be an artifact of the heat denaturation of the samples. The IIF7-reactive bands were absent in dysgenic myotubes (leftmost lane, Fig. 2 A), supporting the conclusion that they represent $Ca_V1.1$.

A clear trend, which is evident in Fig. 2 A, was that the relative abundance of the larger $Ca_V1.1$ protein decreased as a function of in vitro developmental age, an effect that was also present in the averaged data (Fig. 2 B). The decreasing relative abundance of the larger $Ca_V1.1$

was even more pronounced for muscle developing in vivo, declining from ~30% in the first few days after birth to <10% after about 1 mo (Fig. 2 C). This latter is comparable to the fraction of full-length $Ca_V1.1$ reported previously for adult rabbit skeletal muscle (De Jongh et al., 1991). Thus, the posttranslational truncation of $Ca_V1.1$ appears to be similar in mouse and rabbit.

Apparent lack of interaction in muscle cells between the distal $Ca_V1.1$ C-terminal and proximal domains of the channel

To examine further the relationship between the two sizes of mouse $Ca_V1.1$, we generated an antibody against a peptide corresponding to a sequence that is downstream from the rabbit truncation site and is conserved between rabbit and mouse (Fig. 1, "distal Ab"). Fig. 3 compares immunoprecipitation of digitonin-solubilized neonatal muscle membranes with either IIF7 ("Proximal") or the distal antibody. With IIF7, both the larger and smaller $Ca_V1.1$ polypeptides were immunoprecipitated, whereas only the larger polypeptide was immunoprecipitated by the distal antibody. This result demonstrates that the larger polypeptide contains the distal C terminus (i.e., essentially full-length), whereas the shorter polypeptide lacks the distal C terminus (i.e., truncated). However, the results illustrated in Fig. 3 have an additional implication. Specifically, if the cleaved distal C terminus had been bound to the truncated proximal channel, then the distal antibody should have immunoprecipitated both the truncated and nontruncated polypeptides. That this did not occur suggests that the distal C terminus does not bind to the truncated channel in muscle cells.

It is possible that the experiment shown in Fig. 3 failed to detect an interaction between the distal C terminus and proximal $Ca_V1.1$ because this interaction was disturbed by digitonin, or that this proposed interaction masked the epitope for the distal antibody. Thus, we also tested for the interaction by electroporating FDB fibers of adult mice with a construct encoding $Ca_V1.1$ with a CFP-YFP tandem attached to the N terminus (CFP-YFP-$Ca_V1.1$), or with YFP attached to the N terminus and CFP attached to residue 1,860 of the C-terminus (YFP-$Ca_V1.1$-CFP). Subsequently, images were obtained of dissociated fibers displaying a striated yellow fluorescence pattern consistent with a t-tubular localization of the $Ca_V1.1$ construct. Fig. 4 illustrates the patterns observed in one fiber transfected with CFP-YFP-$Ca_V1.1$ (Fig. 4 A) and in two fibers transfected with YFP-$Ca_V1.1$-CFP (Fig. 4, B and C). Fluorescence intensity profiles for these three fibers, within the indicated regions of interest, are shown in Fig. 4 (A′, B′, and C′). The fiber transfected with CFP-YFP-$Ca_V1.1$ displayed colocalized yellow and cyan fluorescence (indicated by red and green, respectively; Fig. 4, A and A′); similar colocalized striations were present in two fibers dissociated 9 d after transfection with CFP-YFP-$Ca_V1.1$ and nine fibers dissociated 14 d after transfection. In contrast, the fibers expressing YFP-$Ca_V1.1$-CFP displayed yellow striations like those of fibers expressing CFP-YFP-$Ca_V1.1$, but not colocalized striations of cyan fluorescence (Fig. 4, B, B′, C, and C′). Rather, some fibers in which YFP-$Ca_V1.1$-CFP was highly expressed displayed obvious cyan fluorescent striations that were offset from the yellow fluorescence (Fig. 4, B and B′), which is the pattern that would be produced if the CFP-tagged distal C terminus had been cleaved and accumulated in the I-bands adjacent to the t-tubules. In other fibers expressing YFP-$Ca_V1.1$-CFP at a lower level (Fig. 4, C and C′), both the yellow and cyan fluorescence were weaker, and the offset striations of cyan fluorescence were either less pronounced or not discernible. Altogether, images were obtained from a total of 11 fibers expressing YFP-$Ca_V1.1$-CFP at either 9 d (three fibers) or 14 d (eight fibers). Out of these 11 fibers, offset cyan striations (like those of Fig. 4, B and C) were present in seven (two at 9 d and five at 14 d), and low level cyan fluorescence with an indeterminate distribution was present in four (one at 9 d and three at 14 d).

Based on the results shown in Figs. 2–4, it appears that in adult skeletal muscle (a) the majority of the distal

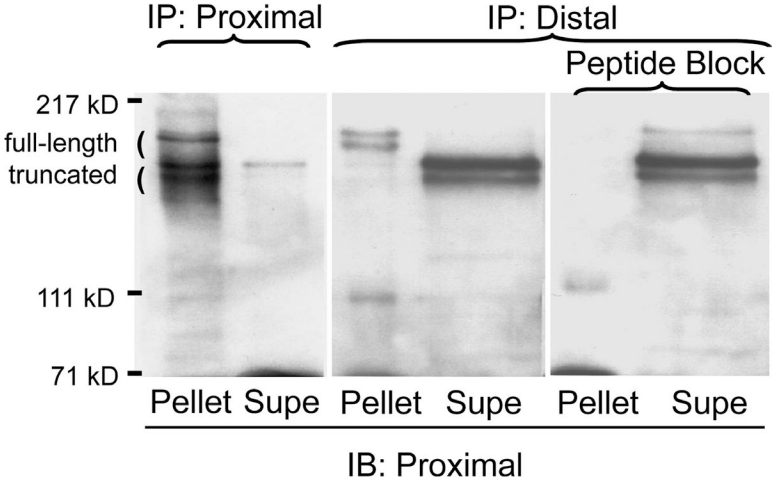

Figure 3. IIF7, which has an epitope proximal to the truncation site, immunoprecipitates both sized species of $Ca_V1.1$, whereas the distal antibody only immunoprecipitates the larger species. Solubilized P1 muscle membranes were immunoprecipitated with either IIF7 (lanes 1 and 2) or with the distal antibody (lanes 3 and 4), or with the distal antibody preincubated with its generating peptide (lanes 5 and 6). Western blotting of the resulting pellets and supernatants with IIF7 demonstrates that the distal epitope is present only in the larger-sized form of $Ca_V1.1$. Note that lanes 3–6 are all from the same experiment, that lanes 3 and 5 were loaded identically, and that lanes 4 and 6 were loaded identically.

C terminus is cleaved, as also indicated by the data in Fig. 2 C; and (b) after cleavage, the distal C terminus does not remain associated with proximal domains of $Ca_V1.1$.

Deletion of >200 residues from the distal C terminus of $Ca_V1.1$ does not alter L-type Ca^{2+} channel activity

To test the functional consequences of C-terminal truncation, we performed electrophysiological measurements. Fig. 5 A illustrates representative whole-cell Ca^{2+} currents after depolarization to the indicated potentials from dysgenic myotubes expressing YFP-$Ca_V1.1_{1860}$ (top) or YFP-$Ca_V1.1_{1666}$ (bottom). Based on average peak current versus voltage relationships (Fig. 5 B), the currents were of virtually identical amplitude and voltage dependence in dysgenic myotubes expressing YFP-$Ca_V1.1_{1666}$ or YFP-$Ca_V1.1_{1860}$. This result is in agreement with earlier results demonstrating that estimated P_o after expression in dysgenic myotubes differs little between untagged $Ca_V1.1$, which is full-length or truncated at residue 1662 (Beam et al., 1992). Moreover, the attachment of a fluorescent protein to the N terminus does not seem to have much effect on channel function because estimated P_o for $Ca_V1.1$ N-terminally tagged with GFP (Grabner et al., 1999) is similar to that of untagged $Ca_V1.1$ (Beam et al., 1992).

The distal C terminal of $Ca_V1.1$ is not necessary for depolarization-induced potentiation of L-type Ca^{2+} current

To analyze the depolarization-induced potentiation of the skeletal L-type Ca^{2+} current, we used two voltage protocols

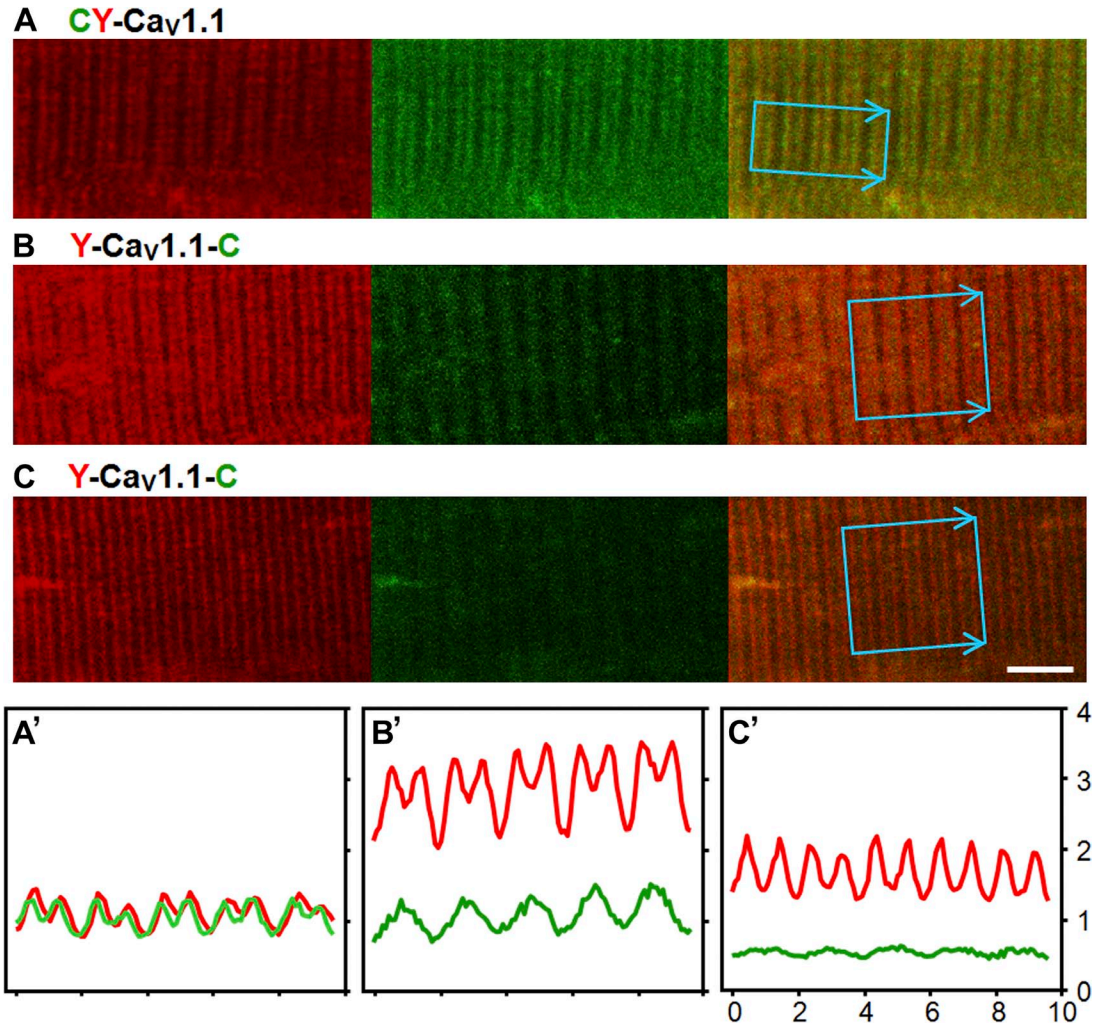

Figure 4. Confocal fluorescence images representative of the patterns observed for CFP-YFP-$Ca_V1.1$ (A) or YFP-$Ca_V1.1$-CFP (B and C) obtained 2 wk after transfection of adult mouse FDB muscle; the yellow and cyan fluorescence are illustrated in red and green, respectively. The images were obtained with identical photomultiplier settings on an LSM710 confocal microscope; the corresponding average intensity profiles, within the indicated regions of interest, are illustrated in A′, B′, and C′, with the horizontal and vertical axes corresponding to micrometer and average pixel intensity ($\times 10^{-3}$), respectively. The intensities in B′ and C′ were scaled according to the ratio of laser intensity (for B or C) to corresponding laser intensity (for A). Thus, the intensity profiles indicate that, compared with the cell illustrated in A and A′, the expression of $Ca_V1.1$ was about threefold higher in B and B′ and ~1.5-fold higher in C and C′. Calibration bar, 5 µm for all panels.

that were similar to those used in previous work (Johnson et al., 1994, 1997). In one protocol (Fig. 6 A, top), 200-ms steps to increasingly depolarized potentials were applied, followed by repolarization to elicit inward tail current. In the other protocol (Fig. 6 B, top), the duration of a depolarization to 90 mV was varied from 50 to 200 ms, before repolarization. As shown in Fig. 6, tail current amplitude was increased and decay time slowed when the prepulse depolarization was made either larger (Fig. 6, A and B) or longer (Fig. 6, C and D). This behavior is similar to that described previously for myotubes produced from the 129CB3 line of immortalized mouse myoblasts (Johnson et al., 1994, 1997). Importantly, the effects of increased prepulse amplitude, and of increased prepulse duration, were qualitatively similar in dysgenic myotubes expressing either $Ca_V1.1_{1860}$ or $Ca_V1.1_{1666}$.

Four different quantities were used to compare depolarization-induced potentiation in dysgenic myotubes expressing YFP-$Ca_V1.1_{1860}$ or YFP-$Ca_V1.1_{1666}$. These were: (1) I_{90}/I_{40}, where the numerator and denominator represent peak inward tail currents elicited by repolarization after a 200-ms depolarization to either 90 or 40 mV (Fig. 7 A1); (2) I_{200}/I_{50}, where the numerator and denominator represent peak inward tail currents elicited by repolarization after a 90-mV depolarization of either 200 or 50 ms (Fig. 7 B1); (3) T_{90}/T_{40}, where the numerator and denominator represent half-decay times of tail currents elicited by repolarization after a 200-ms depolarization to either 90 or 40 mV (Fig. 7 A2); and (4) T_{200}/T_{50}, where the numerator and denominator represent half-decay times of tail currents elicited by repolarization after a 90-mV depolarization of either 200 or 50 ms (Fig. 7 B2). There was no statistically significant difference ($P > 0.05$) in any of these four measures between dysgenic myotubes expressing YFP-$Ca_V1.1_{1860}$ or YFP-$Ca_V1.1_{1666}$.

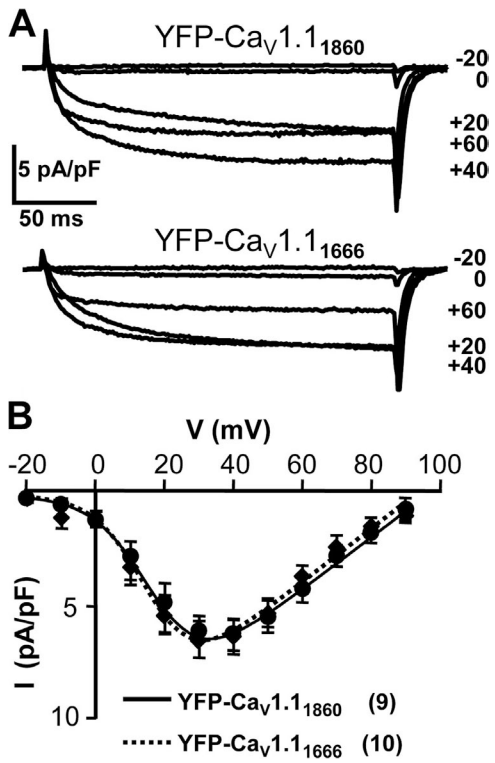

Figure 5. Ca^{2+} currents produced by expression in dysgenic myotubes of rabbit YFP-$Ca_V1.1_{1860}$ or of YFP-$Ca_V1.1_{1666}$ lacking the distal C terminus. In vivo, proteolytic cleavage has been reported to sever after residue 1,664 (Hulme et al., 2005). (A) Representative currents from dysgenic myotubes expressing cDNA encoding either YFP-$Ca_V1.1_{1860}$ (top) or YFP-$Ca_V1.1_{1666}$ (bottom), elicited by 200-ms depolarization to the indicated potentials. (B) Average peak current versus voltage relationships for YFP-$Ca_V1.1_{1860}$ (●) and YFP-$Ca_V1.1_{1666}$ (◆), with the number of experiments given in parentheses. The smooth curves represent plots of Eq. 1, with the average values determined by best fits to the data from individual cells. Error bars indicate ± SEM.

In addition to examining the effects of truncation by comparing dysgenic myotubes after transfection with YFP-$Ca_V1.1_{1860}$ or YFP-$Ca_V1.1_{1666}$, we also compared potentiation in muscle fibers from neonatal and 30-d postnatal mice. Over this time period, there was a greater than fourfold decease in the fraction of full-length $Ca_V1.1$ (Fig. 2 C). However, as shown in Fig. 8, depolarization-induced potentiation did not differ significantly in fibers from neonatal and 30-d postnatal mice.

DISCUSSION

In this study, we examined the posttranslational processing of the $Ca_V1.1$ C terminus, and whether the distal C terminus is required for depolarization-induced potentiation of the L-type Ca^{2+} current in skeletal muscle. In agreement with previous work (De Jongh et al., 1991), we found two different sizes of $Ca_V1.1$, with the smaller one constituting the majority (>90%) in adult mouse skeletal muscle; additionally, we found that relative abundance of this smaller form increased during postnatal development (Fig. 2). Based on immunoprecipitation, the larger form contains a "distal" epitope which is <50 residues from the predicted termination of mouse $Ca_V1.1$ (Fig. 1), whereas the smaller form lacks this epitope (Fig. 3), which is consistent with the idea that truncation of mouse $Ca_V1.1$ is homologous to that experimentally determined for rabbit $Ca_V1.1$ (Hulme et al., 2005; Fig. 1). Two experimental approaches indicated that the distal portion of the C terminus does not remain noncovalently bound to proximal $Ca_V1.1$. First, an antibody to the distal epitope immunoprecipitated only the larger sized $Ca_V1.1$ from neonatal mouse muscle (Fig. 3). Second, colocalized cyan and yellow fluorescence were not observed after in vivo expression in adult FDB fibers of YFP-$Ca_V1.1$-CFP (Fig. 4). Rather, the yellow fluorescence appeared to reflect a t-tubular location, whereas the cyan fluorescence was that which would be expected

if proteolytic cleavage had allowed the movement of the distal C terminus into the myoplasm (predominantly within the I band). Functionally, the analysis of myotubes indicated that the distal C terminus was not important for depolarization-induced potentiation of $Ca_V1.1$ In particular, depolarization-induced potentiation was similar for YFP-$Ca_V1.1_{1860}$ and YFP-$Ca_V1.1_{1666}$ expressed in dysgenic myotubes (Fig. 7). Additionally, depolarization-induced potentiation differed little between neonatal and postnatal day 30 muscle fibers (Fig. 8), despite the large change in C-terminal truncation that occurred over this time period (Fig. 2). Because $Ca_V1.1$ can undergo depolarization-induced potentiation without the distal C-terminal domain, it would appear that this potentiation does not require either phosphorylation of serine 1854 or AKAP tethering, within this domain (Fig. 1).

For our analysis of fluorescently tagged $Ca_V1.1$ expressed in FDB muscles (Fig. 4), we primarily examined fibers 2 wk after electroporation, which we selected because it was the earliest of the times used in a previous study of FDB fibers electroporated with $Ca_V1.1$ cDNAs (DiFranco et al., 2011). Based on Western blotting and the measurement of calcium currents, charge movements, and excitation–contraction coupling Ca^{2+} release, DiFranco et al. concluded that in fibers 2–7 wk after electroporation, the exogenously expressed $Ca_V1.1$ constructs replaced the majority of the endogenous $Ca_V1.1$ and functionally interacted with RyR1, and that total $Ca_V1.1$ content (exogenous plus endogenous) was only modestly elevated (37%) compared with fibers that had not been electroporated. Thus, their work implies that the posttranslational processing of the exogenous $Ca_V1.1$ constructs is similar to that of endogenous $Ca_V1.1$.

Because the intensity profiles illustrated for YFP-$Ca_V1.1$-CFP in Fig. 4 (B′ and C′) were scaled relative to that for CFP-YFP-$Ca_V1.1$ (Fig. 4 A′) to account for differences in laser excitation intensity, the yellow intensity profiles in the three panels should be directly comparable to one another, as should the cyan intensity profiles. Furthermore, if CFP and YFP are assumed to be equimolar in fibers expressing CFP-YFP-$Ca_V1.1$, then the ratio of the cyan to yellow fluorescence in Fig. 4 (B′ and C′) should reflect the abundance of the CFP-tagged C terminus relative to that of the YFP-tagged proximal $Ca_V1.1$. (The agreement in the average yellow and cyan intensities in Fig. 4 A′ is a consequence of the

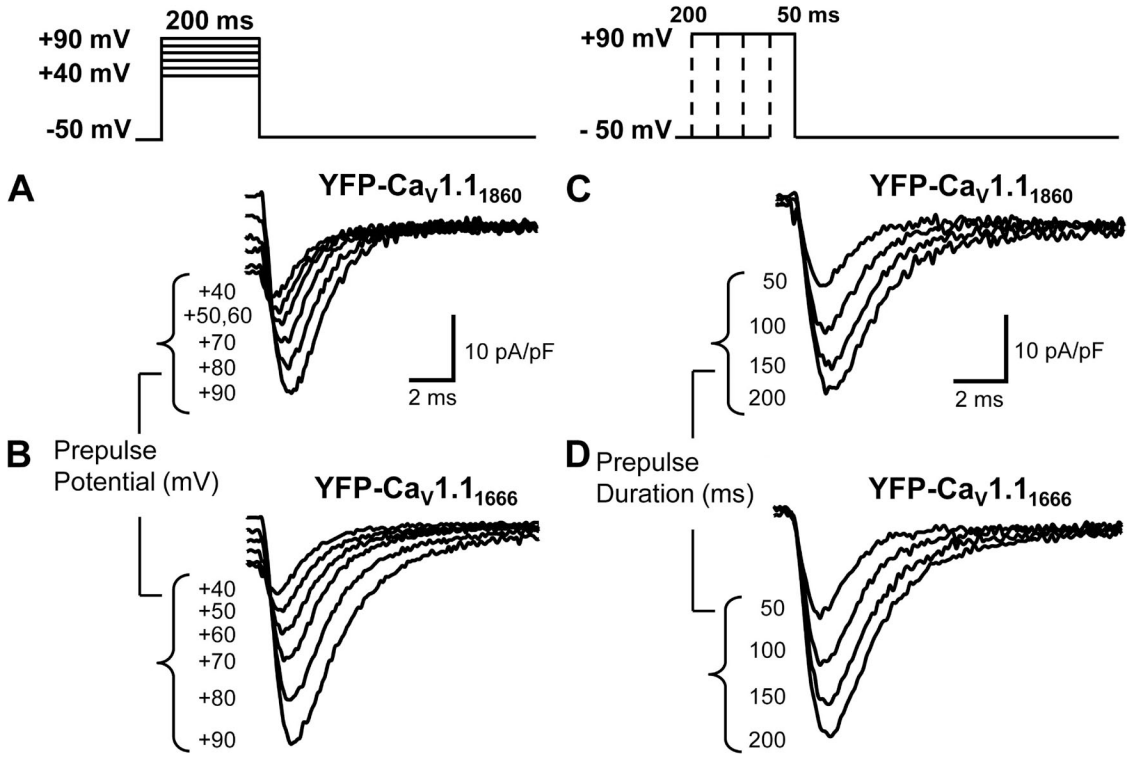

Figure 6. Potentiation by strong depolarization is qualitatively similar for $Ca_V1.1_{1860}$ and $Ca_V1.1_{1666}$. Potentiation was assayed by measuring tail currents upon repolarization to −20 mV after 200-ms prepulses of varying potential (A and B), or after prepulses to 90 mV of varying duration (C and D). These protocols are illustrated at the top of the figure, and the prepulse potentials or durations are indicated adjacent to the tail currents. Increasing either the potential or duration of the prepulse caused tail current amplitude to increase and decay to slow in a similar manner for dysgenic myotubes expressing cDNA encoding either $Ca_V1.1_{1860}$ (A and C) or $Ca_V1.1_{1666}$ (B and D).

specific laser and photomultiplier settings used, and does not directly imply an equimolar presence of CFP and YFP.) However, if CFP and YFP are assumed equimolar in fibers expressing CFP-YFP-$Ca_V1.1$, then the cyan and yellow intensity profiles in B′ and C′ provide a direct estimate of the abundance of the CFP moiety relative to that of the YFP moiety in these two fibers expressing YFP-$Ca_V1.1$-CFP. By this interpretation, the spatially averaged concentration of the CFP-tagged C-terminal fragment relative to the rest of the channel is ~38 and ~33% for the profiles in Fig. 4 (B′ and C, respectively). We have not investigated the mechanisms responsible for this loss of the CFP-tagged fragment, although proteolysis and diffusion into regions of the fibers not producing the YFP-$Ca_V1.1$-CFP protein are both possibilities. Nonetheless, one might expect that the residual level of CFP-tagged C terminus would have been sufficient to result in colocalized CFP and YFP striations if it had bound to the proximal channel. Of course, we cannot exclude the possibility that the stability of the postulated interaction between the distal C terminus and proximal $Ca_V1.1$ was affected by the presence of the C-terminal fluorescent protein.

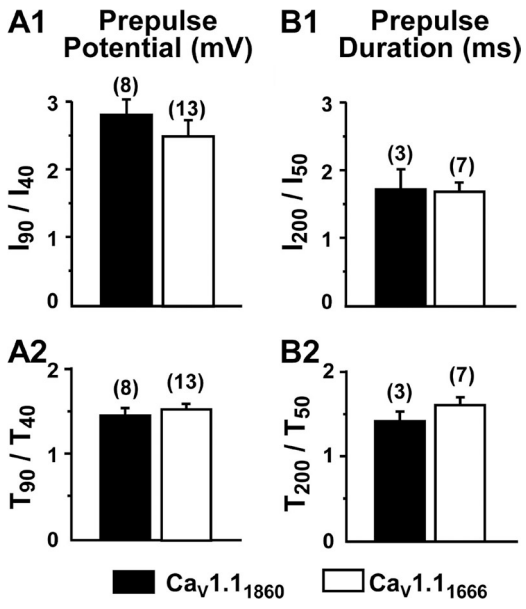

Figure 7. Potentiation is quantitatively similar for $Ca_V1.1_{1860}$ and $Ca_V1.1_{1666}$. Both the amplitude (I) and half-decay time (T) were measured for tail currents upon repolarization after either 200-ms prepulses to 40 or 90 mV (A1 and A2), or after 90-mV prepulses of 50- or 200-ms duration (B1 and B2). The number of cells examined is indicated in parentheses. There were no statistically significant differences between $Ca_V1.1_{1860}$ and $Ca_V1.1_{1666}$ based on a rank-sum test (I_{90}/I_{40}, P = 0.205; I_{200}/I_{50}, P = 1.0) or *t* test (T_{90}/T_{40}, P = 0.486; T_{200}/T_{50}, P = 0.289). Tail current repolarization potential was −20 mV for $Ca_V1.1_{1860}$ and ranged from −20 to −40 mV for $Ca_V1.1_{1666}$ (see Materials and methods).

Comparison with other studies of $Ca_V1.1$ potentiation

To compare our results on $Ca_V1.1$ potentiation with those of previous studies, it is necessary to take differences of experimental conditions into account. For example, Johnson et al. (1997) used an external solution containing 10 mM Ba^{2+} to measure tail currents at −80 mV after 500-ms depolarizations ranging from −40 mV up to either 60 or 80 mV. Tail current amplitudes and decay times were found to increase over this entire range, presumably as a result of increasing contributions from: (a) "OFF"-gating currents largely attributable to $Ca_V1.1$; (b) inward ionic (Ba^{2+}) current resulting from the increasing activation of nonpotentiated $Ca_V1.1$ channels; and (c) inward ionic currents produced by potentiated $Ca_V1.1$ channels. To examine voltage-dependent potentiation of $Ca_V1.1$, in our work, we used a less negative repolarization potential. We also tried to minimize contributions (a) and (b) by comparing tail currents after depolarizing test potentials above 40 mV (where both OFF-gating currents and conventional [nonpotentiated] activation are near or at saturation under our experimental conditions; compare Bannister et al., 2008). We found that for neonatal muscle fibers, I_{90}/I_{40} (Fig. 8 A1) and T_{90}/T_{40} (Fig. 8 A2) had values of ~2.8 and ~1.5, respectively. By way of comparison, Johnson et al. (1997) found that tail current amplitude and time constant for tail current decay in mouse myotubes increased ~1.7-fold and approximately twofold, respectively, over the

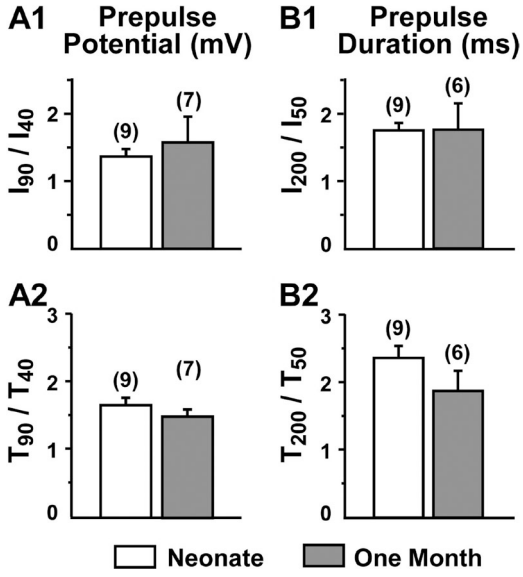

Figure 8. Potentiation is quantitatively similar for native $Ca_V1.1$ in muscle fibers of neonatal (day 0 and day 1) mice and 1-mo-old mice. Potentiation was quantified as illustrated in Figs. 6 and 7 for tail currents produced by repolarization to −30 mV (number of cells in parentheses). *t* test comparisons of potentiation in dissociated FDB muscle fibers from neonatal and 1-mo-old mice yielded P = 0.23 for I_{90}/I_{40} (A1), P = 0.39 for T_{90}/T_{40} (A2), P = 0.90 for I_{200}/I_{50} (B1), and P = 0.19 for T_{200}/T_{50} (B2).

most comparable voltage range illustrated in their Fig. 2 C (between 10 and 60 mV). It should be noted that because 10 mM Ba^{2+} produces an ~10-mV hyperpolarizing shift in the activation of current via $Ca_V1.1$ compared with 10 mM Ca^{2+} (Beam and Knudson, 1988), those voltages would correspond approximately to 20 and 70 mV under our experimental conditions. Thus, the potentiation by strong depolarization found in our work appears to be in reasonably good quantitative agreement with that found by Johnson et al. (1997).

Johnson et al. (1997) additionally determined how tail current amplitudes and decay times were affected by varying the duration of an 80-mV prepulse from 5 to 75 ms, whereas we varied a 90-mV prepulse from 50 to 200 ms. We chose these longer durations because one might reasonably expect that between 5 and 50 ms, the increasing activation of $Ca_V1.1$ liter-type current (compare Fig. 5 A) would cause a large change in the subsequent tail currents, even if there were no potentiation occurring over this time interval. Nonetheless, the fold-change found by Johnson et al. (1997) in tail current amplitude (~1.4) and decay time (~2) for control mouse myotubes between 50 and 75 ms (closed circles in their Fig. 3, C and D) are roughly comparable to the values that we found of ~1.7 for I_{200}/I_{50} (Fig. 8 B1) and of ~1.5 for T_{200}/T_{50} (Fig. 8 B2).

The effects of strong depolarization on Ca^{2+} currents in mouse myotubes has also been examined with a much different protocol (Hulme et al., 2002). Specifically, a "conditioning sequence," which consisted of a 200-ms potentiating prepulse to 100 mV followed by a 25-ms repolarization to −60 mV, was applied before depolarizing test pulses to varying levels. The presence of this intervening hyperpolarization, which would cause channels to deactivate, means that the subsequent test pulse assayed channels that were predominantly closed, unlike the tail current protocol used by us and by Johnson et al. (1997), which assayed channels that were open at the end of the potentiating prepulse. When Hulme et al. (2002) compared currents for the test depolarizations that were preceded by the conditioning sequence, with currents elicited by the identical depolarizations applied directly from the holding potential (−80 mV), they found that the effects of the conditioning sequence depended strongly on test potential (their Fig. 6). Specifically, the test currents were increased for test potentials within the negative slope region of the peak I-V relationship (roughly −20 to 10 mV, with the biggest effect at more negative potentials) but were little altered for test potentials ≥20 mV. This behavior indicates that the phenomenon studied by Hulme et al. (2002) is mechanistically different from that characterized here and in Johnson et al. (1997). Indeed, we found that when potential was stepped directly from a strongly depolarizing prepulse, current amplitudes increased greatly when the subsequent pulse was either to a hyperpolarized level (Fig. 6) or to a depolarized level (30 mV; Fig. 4 e of Tanabe et al., 1991).

Is full-length $Ca_V1.1$ present in the plasma membrane?

$Ca_V1.1$ channel P_o's have been estimated from measurements of peak ionic currents and of gating charge movements (the latter as an indicator of membrane expression). With this approach, estimated P_o was found not to differ after expression in dysgenic myotubes of cDNAs encoding full-length or truncated (at residue 1662) $Ca_V1.1$ (Beam et al., 1992). One possible explanation for the similarity of estimated P_o is that even when myotubes are transfected with cDNA encoding full-length $Ca_V1.1$, truncation occurs before insertion into the plasma membrane. However, an argument against this idea is provided by experiments in which a $Ca_V1.1$-GFP construct was transiently expressed in dysgenic myotubes (Flucher et al., 2000), followed by fixation, permeabilization, and double immunostaining with a monoclonal antibody against the $Ca_V1.1$ II–III loop (Kugler et al., 2004) and an anti-GFP polyclonal antibody. With this approach, staining with the two antibodies was observed to colocalize in discrete puncta, as would be produced by the membrane insertion of full-length channels, but the methodology does not provide a quantitative estimate of what fraction of membrane-inserted $Ca_V1.1$ was full-length and what fraction was truncated. However, if the experiments on *Xenopus* oocytes are taken as a guide, it would seem that the fraction of membrane-inserted, full-length $Ca_V1.1$ must be quite small. In particular, estimated P_o is about fivefold lower for full-length rabbit $Ca_V1.1$ expressed in *Xenopus* oocytes than for $Ca_V1.1$ truncated at residue 1697 (Morrill and Cannon, 2000). If this also applied to myotubes and if half of all $Ca_V1.1$ in the membrane were full-length, then estimated P_o would be 40% lower after expression of full-length $Ca_V1.1$ in myotubes than after expression of truncated $Ca_V1.1$, which is clearly not the case (Beam et al., 1992). However, if the fraction of full-length $Ca_V1.1$ were relatively small (20%, say), then the estimated P_o would be reduced only ~15%, which would make it difficult to distinguish between myotubes transfected with full-length or truncated constructs. Of course, one must also take into account that the regulation of P_o differs between myotubes and oocytes. For example, RyR1, which is present in myotubes but not in oocytes, causes an approximate threefold increase in P_o of the endogenous $Ca_V1.1$ Ca^{2+} channels in mouse myotubes (Nakai et al., 1996).

Whether or not full-length channels can insert into the plasma membrane, our results make it clear that depolarization-induced potentiation can occur in the complete absence of the distal C terminus. Moreover, potentiation was quantitatively similar for YFP-$Ca_V1.1_{1860}$ and YFP-$Ca_V1.1_{1666}$ (Fig. 7). In principle, potentiation of YFP-$Ca_V1.1_{1860}$ could differ from that of full-length $Ca_V1.1$

because of the absence of the final 13 residues. However, it seems unlikely that these terminal residues are of major importance, as there is only modest conservation of sequence in this region between rabbit and mouse $Ca_V1.1$ (Fig. 1), and potentiation of Ca^{2+} current in wild-type mouse FDB muscle fibers (Fig. 8) is not much different from that in dysgenic myotubes expressing the rabbit constructs (Fig. 7).

Biological role of $Ca_V1.1$ distal C terminus

Our current results raise once again the question of the role of the distal C terminus of $Ca_V1.1$. In particular, a truncated $Ca_V1.1$ is able to function as both L-type Ca^{2+} channel and voltage sensor for excitation–contraction coupling (Beam et al., 1992), and to undergo depolarization-induced potentiation, without need for the distal segment of the C terminus (Figs. 6–8). It is possible that the distal C terminus is important for the regulation of Ca^{2+} current via $Ca_V1.1$ in response to β-adrenergic activation of the PKA pathway in skeletal muscle, as has been proposed for $Ca_V1.2$ in heart (Fuller et al., 2010). However, the effect of activating PKA in skeletal muscle appears to be very modest, amounting to 25% or less in mouse myotubes (Fratacci et al., 1996; Held et al., 2002). Furthermore, we could find no evidence of an association in muscle cells between the distal C terminus and proximal $Ca_V1.1$, as probed both by immunoprecipitation and by expression of fluorescently tagged $Ca_V1.1$. In light of these results, one could postulate that the primary role of the distal C terminus is to act as a regulator of the insertion of $Ca_V1.1$ into the plasma membrane (i.e., that its removal promotes this insertion). This hypothesis might account for why the C-terminal sequence is conserved between mouse and rabbit in the region surrounding the site of posttranslational truncation, but not for why there is also considerable conservation within the distal C terminus of the proposed AKAP-binding domain and the "distal C terminus interaction domain," as indicated by the green and red lines, respectively, in Fig. 1. Thus, it seems likely that there are other biological roles for the distal C terminus. One possibility is that it functions as a transcriptional regulator, as has been suggested for the distal C terminus of $Ca_V1.2$ (Gomez-Ospina et al., 2006; Schroder et al., 2009). Alternatively, it might help to regulate the insertion and removal pathways that govern the homeostasis of $Ca_V1.1$ levels in the plasma membrane. Exploration of these potential roles would be aided by information about where and how the posttranslational truncation occurs and perhaps by creation of knock-in mice with a stop codon placed at the truncation site.

We acknowledge the contributions of Deborah Shulman in producing the Western blots used in Figs. 1 and 2. We thank Dr. K.P. Campbell for providing the IIF7 monoclonal antibody.

This work was supported by grants from the National Institutes of Health (AR055104) and the Muscular Dystrophy Association (MDA176448) to K.G. Beam, and the American Heart Association (9100126G) to J.D. Ohrtman.

The authors declare no competing financial interests.

Angus C. Nairn served as editor.

Submitted: 19 September 2014
Accepted: 27 February 2015

REFERENCES

Bannister, R.A., H.M. Colecraft, and K.G. Beam. 2008. Rem inhibits skeletal muscle EC coupling by reducing the number of functional L-type Ca^{2+} channels. *Biophys. J.* 94:2631–2638. http://dx.doi.org/10.1529/biophysj.107.116467

Beam, K.G., and C. Franzini-Armstrong. 1997. Functional and structural approaches to the study of excitation-contraction coupling. *Methods Cell Biol.* 52:283–306. http://dx.doi.org/10.1016/S0091-679X(08)60384-2

Beam, K.G., and C.M. Knudson. 1988. Calcium currents in embryonic and neonatal mammalian skeletal muscle. *J. Gen. Physiol.* 91:781–798. http://dx.doi.org/10.1085/jgp.91.6.781

Beam, K.G., B.A. Adams, T. Niidome, S. Numa, and T. Tanabe. 1992. Function of a truncated dihydropyridine receptor as both voltage sensor and calcium channel. *Nature.* 360:169–171. http://dx.doi.org/10.1038/360169a0

De Jongh, K.S., C. Warner, A.A. Colvin, and W.A. Catterall. 1991. Characterization of the two size forms of the alpha 1 subunit of skeletal muscle L-type calcium channels. *Proc. Natl. Acad. Sci. USA.* 88:10778–10782. http://dx.doi.org/10.1073/pnas.88.23.10778

De Jongh, K.S., B.J. Murphy, A.A. Colvin, J.W. Hell, M. Takahashi, and W.A. Catterall. 1996. Specific phosphorylation of a site in the full-length form of the alpha 1 subunit of the cardiac L-type calcium channel by adenosine 3′,5′-cyclic monophosphate-dependent protein kinase. *Biochemistry.* 35:10392–10402. http://dx.doi.org/10.1021/bi953023c

DiFranco, M., J. Capote, M. Quiñonez, and J.L. Vergara. 2007. Voltage-dependent dynamic FRET signals from the transverse tubules in mammalian skeletal muscle fibers. *J. Gen. Physiol.* 130:581–600. http://dx.doi.org/10.1085/jgp.200709831

DiFranco, M., P. Tran, M. Quiñonez, and J.L. Vergara. 2011. Functional expression of transgenic α1sDHPR channels in adult mammalian skeletal muscle fibres. *J. Physiol.* 598:1421–1442.

Emrick, M.A., M. Sadilek, K. Konoki, and W.A. Catterall. 2010. Beta-adrenergic-regulated phosphorylation of the skeletal muscle Ca(V)1.1 channel in the fight-or-flight response. *Proc. Natl. Acad. Sci. USA.* 107:18712–18717. http://dx.doi.org/10.1073/pnas.1012384107

Flucher, B.E., N. Kasielke, U. Gerster, B. Neuhuber, and M. Grabner. 2000. Insertion of the full-length calcium channel $\alpha_{(1S)}$ subunit into triads of skeletal muscle in vitro. *FEBS Lett.* 474:93–98. http://dx.doi.org/10.1016/S0014-5793(00)01583-0

Fratacci, M.D., T. Shimahara, R. Bournaud, and G. Atlan. 1996. cAMP-dependent modulation of L-type calcium currents in mouse diaphragmatic cells. *Respir. Physiol.* 104:1–9. http://dx.doi.org/10.1016/0034-5687(96)00031-X

Fuller, M.D., M.A. Emrick, M. Sadilek, T. Scheuer, and W.A. Catterall. 2010. Molecular mechanism of calcium channel regulation in the fight-or-flight response. *Sci. Signal.* 3:ra70. http://dx.doi.org/10.1126/scisignal.2001152

Gao, T., A.E. Cuadra, H. Ma, M. Bünemann, B.L. Gerhardstein, T. Cheng, R.T. Eick, and M.M. Hosey. 2001. C-terminal fragments of the alpha 1C ($Ca_V1.2$) subunit associate with and regulate L-type calcium channels containing C-terminal-truncated alpha 1C subunits. *J. Biol. Chem.* 276:21089–21097. http://dx.doi.org/10.1074/jbc.M008000200

Gomez-Ospina, N., F. Tsuruta, O. Barreto-Chang, L. Hu, and R. Dolmetsch. 2006. The C terminus of the L-type voltage-gated calcium channel Ca(V)1.2 encodes a transcription factor. *Cell.* 127:591–606. http://dx.doi.org/10.1016/j.cell.2006.10.017

Grabner, M., R.T. Dirksen, N. Suda, and K.G. Beam. 1999. The II-III loop of the skeletal muscle dihydropyridine receptor is responsible for the bi-directional coupling with the ryanodine receptor. *J. Biol. Chem.* 274:21913–21919. http://dx.doi.org/10.1074/jbc.274.31.21913

Hamill, O.P., A. Marty, E. Neher, B. Sakmann, and F.J. Sigworth. 1981. Improved patch-clamp techniques for high-resolution current recording from cells and cell-free membrane patches. *Pflugers Arch.* 391:85–100. http://dx.doi.org/10.1007/BF00656997

Held, B., D. Freise, M. Freichel, M. Hoth, and V. Flockerzi. 2002. Skeletal muscle L-type Ca^{2+} current modulation in gamma1-deficient and wildtype murine myotubes by the gamma1 subunit and cAMP. *J. Physiol.* 539:459–468. http://dx.doi.org/10.1113/jphysiol.2001.012745

Hulme, J.T., M. Ahn, S.D. Hauschka, T. Scheuer, and W.A. Catterall. 2002. A novel leucine zipper targets AKAP15 and cyclic AMP-dependent protein kinase to the C terminus of the skeletal muscle Ca^{2+} channel and modulates its function. *J. Biol. Chem.* 277:4079–4087. http://dx.doi.org/10.1074/jbc.M109814200

Hulme, J.T., T.W. Lin, R.E. Westenbroek, T. Scheuer, and W.A. Catterall. 2003. Beta-adrenergic regulation requires direct anchoring of PKA to cardiac $Ca_V1.2$ channels via a leucine zipper interaction with A kinase-anchoring protein 15. *Proc. Natl. Acad. Sci. USA.* 100:13093–13098. http://dx.doi.org/10.1073/pnas.2135335100

Hulme, J.T., K. Konoki, T.W. Lin, M.A. Gritsenko, D.G. Camp II, D.J. Bigelow, and W.A. Catterall. 2005. Sites of proteolytic processing and noncovalent association of the distal C-terminal domain of $Ca_V1.1$ channels in skeletal muscle. *Proc. Natl. Acad. Sci. USA.* 102:5274–5279. http://dx.doi.org/10.1073/pnas.0409885102

Hulme, J.T., V. Yarov-Yarovoy, T.W. Lin, T. Scheuer, and W.A. Catterall. 2006. Autoinhibitory control of the $Ca_V1.2$ channel by its proteolytically processed distal C-terminal domain. *J. Physiol.* 576:87–102. http://dx.doi.org/10.1113/jphysiol.2006.111799

Johnson, B.D., T. Scheuer, and W.A. Catterall. 1994. Voltage-dependent potentiation of L-type Ca^{2+} channels in skeletal muscle cells requires anchored cAMP-dependent protein kinase. *Proc. Natl. Acad. Sci. USA.* 91:11492–11496. http://dx.doi.org/10.1073/pnas.91.24.11492

Johnson, B.D., J.P. Brousal, B.Z. Peterson, P.A. Gallombardo, G.H. Hockerman, Y. Lai, T. Scheuer, and W.A. Catterall. 1997. Modulation of the cloned skeletal muscle L-type Ca^{2+} channel by anchored cAMP-dependent protein kinase. *J. Neurosci.* 17:1243–1255.

Knudson, C.M., N. Chaudhari, A.H. Sharp, J.A. Powell, K.G. Beam, and K.P. Campbell. 1989. Specific absence of the alpha 1 subunit of the dihydropyridine receptor in mice with muscular dysgenesis. *J. Biol. Chem.* 264:1345–1348.

Kugler, G., M. Grabner, J. Platzer, J. Striessnig, and B.E. Flucher. 2004. The monoclonal antibody mAB 1A binds to the excitation–contraction coupling domain in the II-III loop of the skeletal muscle calcium channel $\alpha_{(1S)}$ subunit. *Arch. Biochem. Biophys.* 427:91–100. http://dx.doi.org/10.1016/j.abb.2004.04.007

Leung, A.T., T. Imagawa, and K.P. Campbell. 1987. Structural characterization of the 1,4-dihydropyridine receptor of the voltage-dependent Ca^{2+} channel from rabbit skeletal muscle. Evidence for two distinct high molecular weight subunits. *J. Biol. Chem.* 262:7943–7946.

Lorenzon, N.M., C.S. Haarmann, E.E. Norris, S. Papadopoulos, and K.G. Beam. 2004. Metabolic biotinylation as a probe of supramolecular structure of the triad junction in skeletal muscle. *J. Biol. Chem.* 279:44057–44064. http://dx.doi.org/10.1074/jbc.M405318200

Morrill, J.A., and S.C. Cannon. 2000. COOH-terminal truncated α_{1S} subunits conduct current better than full-length dihydropyridine receptors. *J. Gen. Physiol.* 116:341–348. http://dx.doi.org/10.1085/jgp.116.3.341

Nakai, J., R.T. Dirksen, H.T. Nguyen, I.N. Pessah, K.G. Beam, and P.D. Allen. 1996. Enhanced dihydropyridine receptor channel activity in the presence of ryanodine receptor. *Nature.* 380:72–75. http://dx.doi.org/10.1038/380072a0

Papadopoulos, S., V. Leuranguer, R.A. Bannister, and K.G. Beam. 2004. Mapping sites of potential proximity between the dihydropyridine receptor and RyR1 in muscle using a cyan fluorescent protein-yellow fluorescent protein tandem as a fluorescence resonance energy transfer probe. *J. Biol. Chem.* 279:44046–44056. http://dx.doi.org/10.1074/jbc.M405317200

Pietrobon, D., and P. Hess. 1990. Novel mechanism of voltage-dependent gating in L-type calcium channels. *Nature.* 346:651–655. http://dx.doi.org/10.1038/346651a0

Rotman, E.I., K.S. De Jongh, V. Florio, Y. Lai, and W.A. Catterall. 1992. Specific phosphorylation of a COOH-terminal site on the full-length form of the alpha 1 subunit of the skeletal muscle calcium channel by cAMP-dependent protein kinase. *J. Biol. Chem.* 267:16100–16105.

Schroder, E., M. Byse, and J. Satin. 2009. L-type calcium channel C terminus autoregulates transcription. *Circ. Res.* 104:1373–1381. http://dx.doi.org/10.1161/CIRCRESAHA.108.191387

Sculptoreanu, A., E. Rotman, M. Takahashi, T. Scheuer, and W.A. Catterall. 1993a. Voltage-dependent potentiation of the activity of cardiac L-type calcium channel alpha 1 subunits due to phosphorylation by cAMP-dependent protein kinase. *Proc. Natl. Acad. Sci. USA.* 90:10135–10139. http://dx.doi.org/10.1073/pnas.90.21.10135

Sculptoreanu, A., T. Scheuer, and W.A. Catterall. 1993b. Voltage-dependent potentiation of L-type Ca^{2+} channels due to phosphorylation by cAMP-dependent protein kinase. *Nature.* 364:240–243. http://dx.doi.org/10.1038/364240a0

Tanabe, T., H. Takeshima, A. Mikami, V. Flockerzi, H. Takahashi, K. Kangawa, M. Kojima, H. Matsuo, T. Hirose, and S. Numa. 1987. Primary structure of the receptor for calcium channel blockers from skeletal muscle. *Nature.* 328:313–318. http://dx.doi.org/10.1038/328313a0

Tanabe, T., K.G. Beam, J.A. Powell, and S. Numa. 1988. Restoration of excitation-contraction coupling and slow calcium current in dysgenic muscle by dihydropyridine receptor complementary DNA. *Nature.* 336:134–139. http://dx.doi.org/10.1038/336134a0

Tanabe, T., B.A. Adams, S. Numa, and K.G. Beam. 1991. Repeat I of the dihydropyridine receptor is critical in determining calcium channel activation kinetics. *Nature.* 352:800–803. http://dx.doi.org/10.1038/352800a0

Wei, X., A. Neely, A.E. Lacerda, R. Olcese, E. Stefani, E. Perez-Reyes, and L. Birnbaumer. 1994. Modification of Ca^{2+} channel activity by deletions at the carboxyl terminus of the cardiac alpha 1 subunit. *J. Biol. Chem.* 269:1635–1640.